

Supplementary Information

Triethanolamine-assisted surface reconstruction of nickel oxide for efficient oxygen evolution reaction

Jiayun Zhang ^a, Ruth Knibbe ^{b*}, Ian Gentle ^{a*}

^a School of Chemistry and Molecular Biosciences, The University of Queensland, Brisbane, QLD 4072, Australia

^b School of Mechanical and Mining Engineering, The University of Queensland, Brisbane, QLD 4072, Australia

*Correspondence: ruth.knibbe@uq.edu.au; i.gentle@uq.edu.au

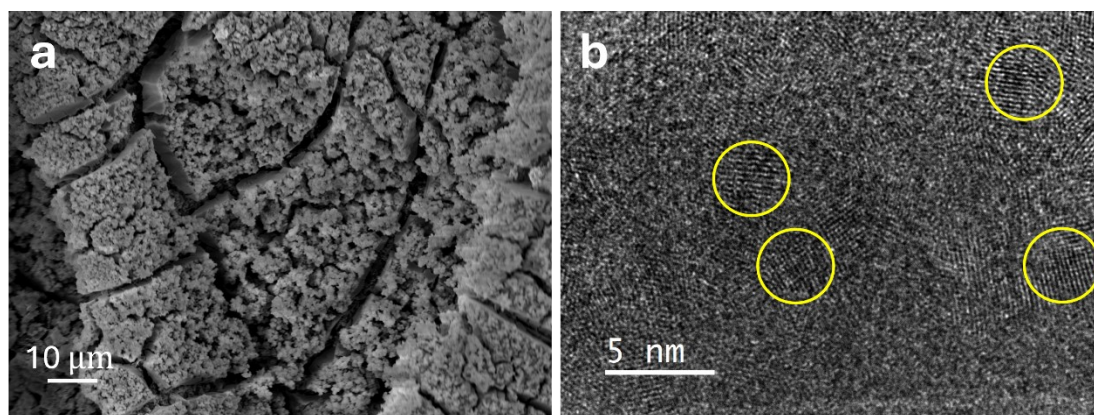


Figure S1. FESEM images of (a) Ni/CP-TEA. (b) and HRTEM images of Ni/CP-TEA.

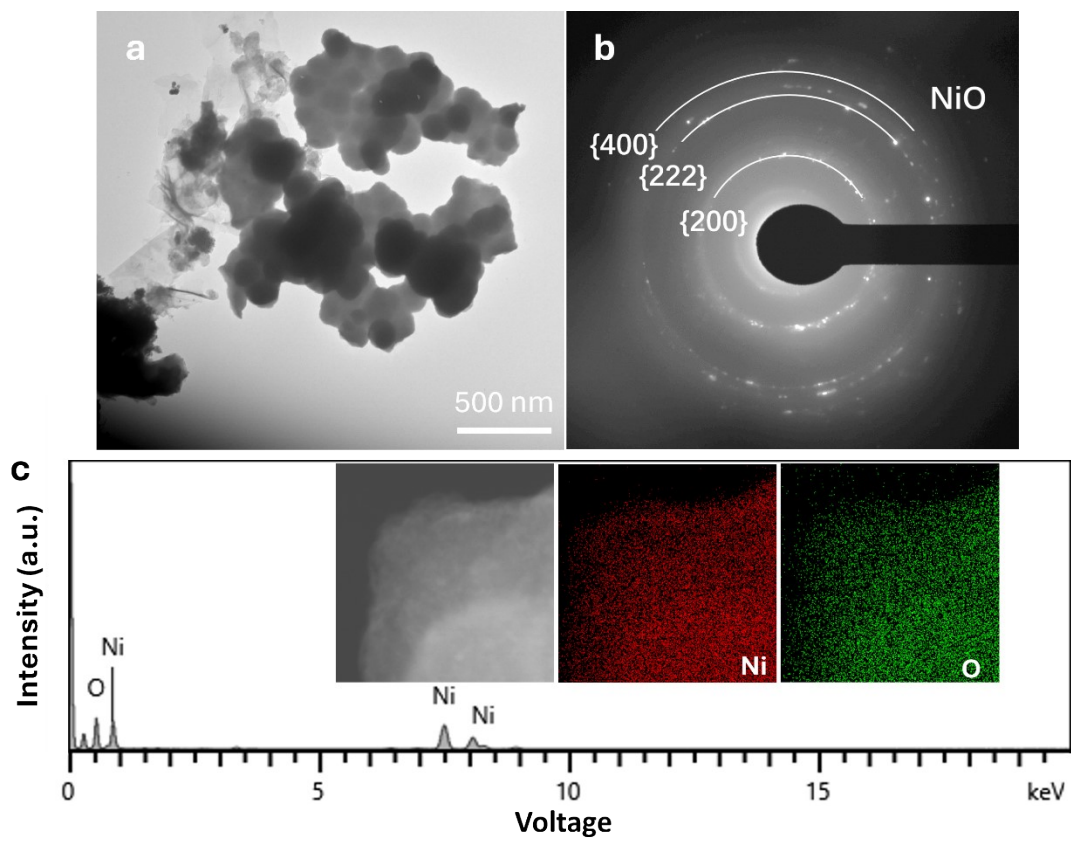


Figure S2. (a) HRTEM image of Ni/CP-TEA and (b) the corresponding SAED pattern. (c) FESEM images a dark field TEM image of Ni/CP-TEA and related elemental mappings.

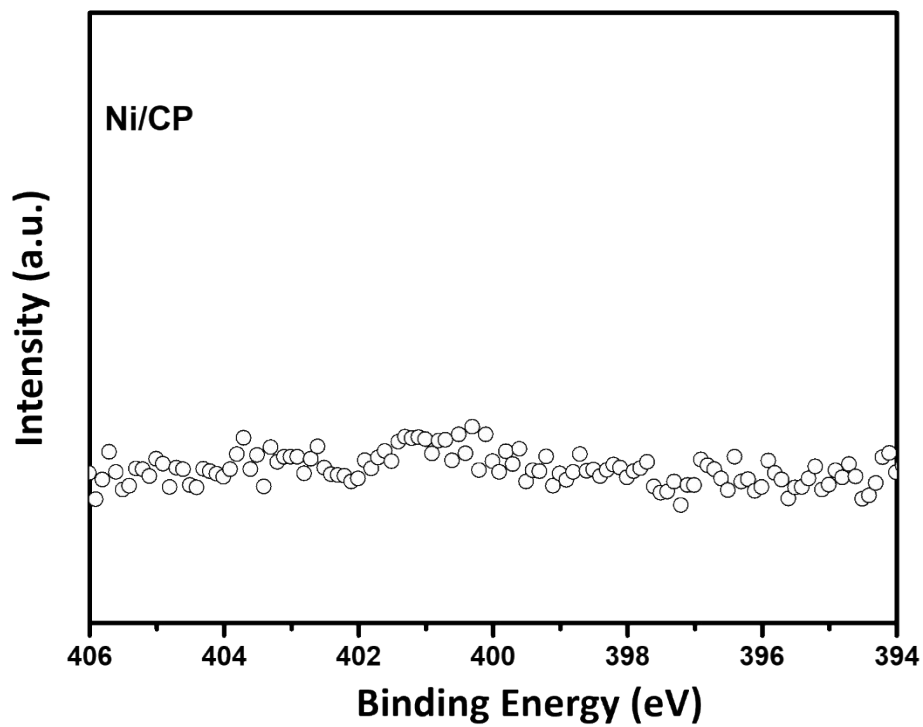


Figure S3. XPS spectra of N 1s region of Ni/CP.

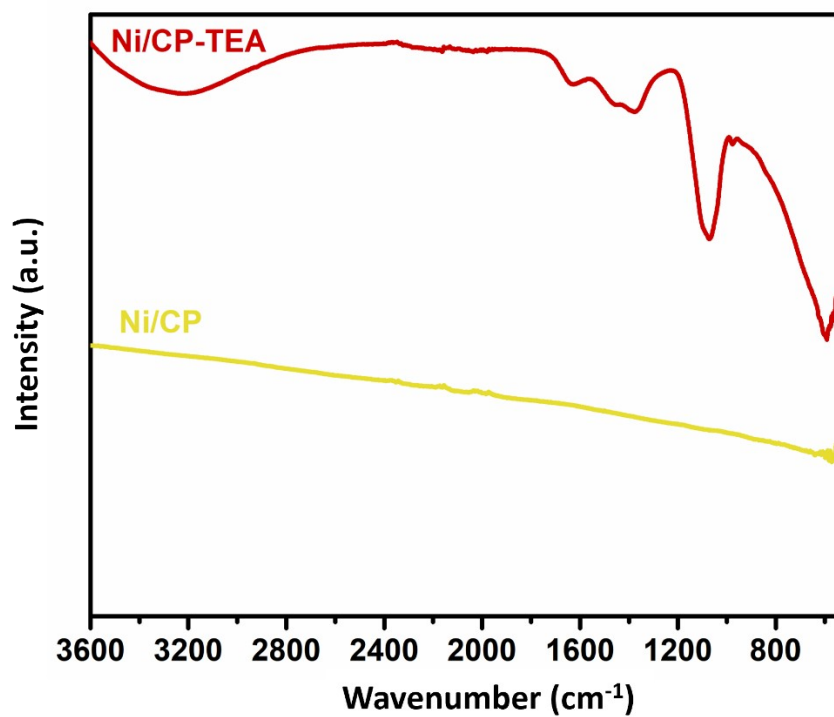


Figure S4. FTIR spectra of Ni/CP-TEA and Ni/CP.

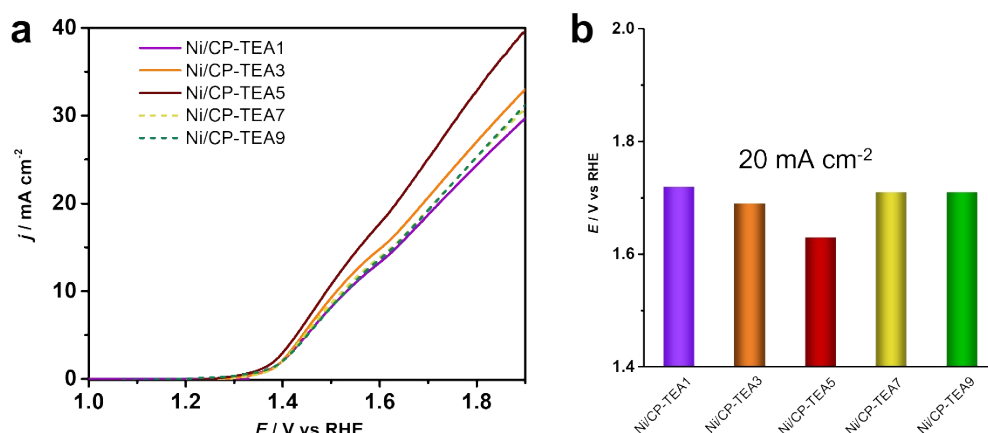


Figure S5. (a) LSV polarization curve of Ni/CP-TEA with different TEA concentrations at $5 \text{ mV}\cdot\text{s}^{-1}$ in 0.1 M KOH and (b) comparison of potential required to achieve a current density of $20 \cdot \text{mA}^{-2}$.

As shown in Figure S5, the activity increased with rising TEA concentration, peaking at 5 mM, before declining. In this work, TEA affects both the morphology and surface chemical structure of the electrocatalyst. Excessive TEA may negatively impact morphology, and increased TEA interactions with surface Ni through Ni-N coordination bonding might influence the reconstruction process, affecting final activity.

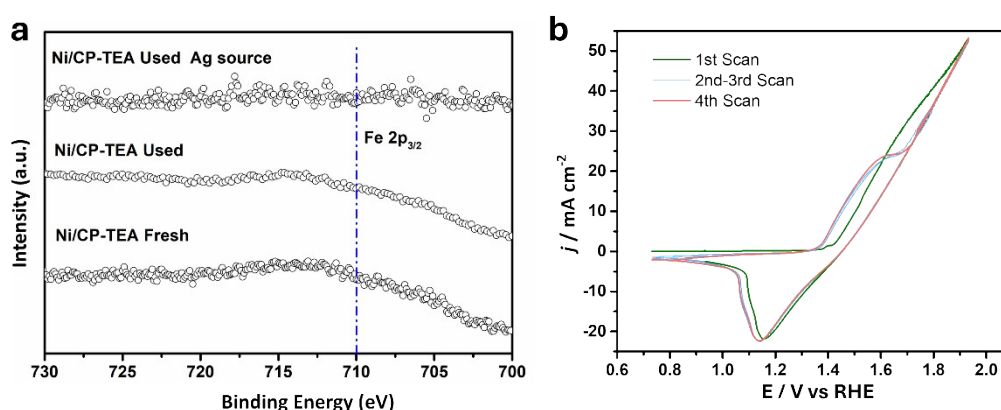


Figure S6. (a) Fe 2p XPS spectra of used Ni/CP-TEA and (b) CV curves of B-Ni/CP-TEA.

Trotochaud et al. investigated the effect of Fe impurities on the changes in electronic properties, OER activity, and structure of $\text{Ni}_{1-x}\text{Fe}_x(\text{OH})_2/\text{Ni}_{1-x}\text{Fe}_x\text{OOH}$.¹ It was reported

that the incorporation of Fe impurities during the CVs or aging period was responsible for the enhanced OER activity observed in some Ni-based electrocatalysts. It was shown that the Fe 2p XPS signal can be detected even after 5 CV cycles in TraceSelect KOH electrolyte (with a Ni/Fe atomic ratio of 95:5). Additionally, the OER activity increased with each CV cycle and the current density increased about 58% after 5 CV cycles. Moreover, aging in either TraceSelect KOH (<36 ppb Fe) or reagent-grade KOH (<1 ppm Fe), further improved OER performance, with positive shifts in both anodic and cathodic peaks.

To clarify the impact of Fe impurities on the Ni/CP-TEA, Fe 2p XPS spectra and CV cycles were measured (Figure S6). As using a typical Al source may cause overlapping of Ni LMM Auger features with Fe 2p peaks, an Ag source was also employed for comparison. As shown in Figure S6a, no Fe 2p signal can be detected for the used Ni/CP-TEA. Additionally, the CV curves (Figure S6b) show a negligible change in OER activity. The negligible change can be also observed in the LSV curve of the Ni/CP-TEA after the stability test (Figure 3c insert). Furthermore, both anodic and cathodic peak positions in the Ni/CP-TEA exhibit negligible shifts after the 2nd CV scan. These results suggest that Fe impurity in electrolyte is not the cause of the enhanced OER performance of the Ni/CP-TEA. The changes in redox peaks and the movement of their positions in CVs between 1st scan and 2nd scan are likely attributed to surface reconstruction.

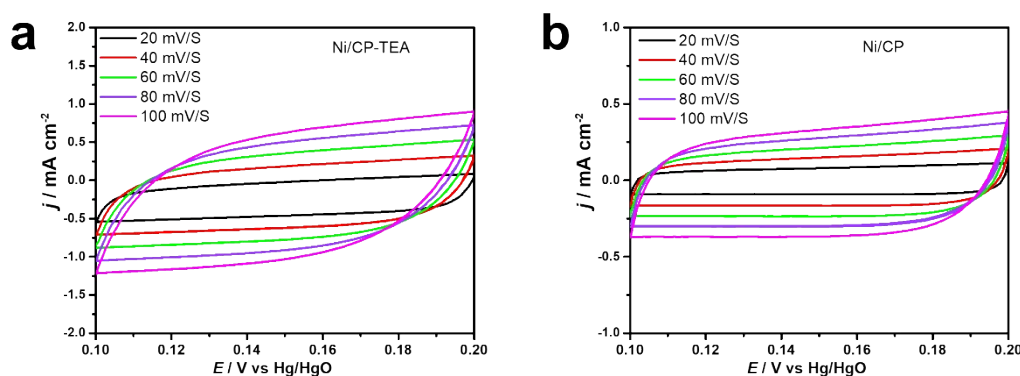


Figure S7. CV curves of different scan rates for (a) Ni/CP-TEA and (b) Ni/CP.

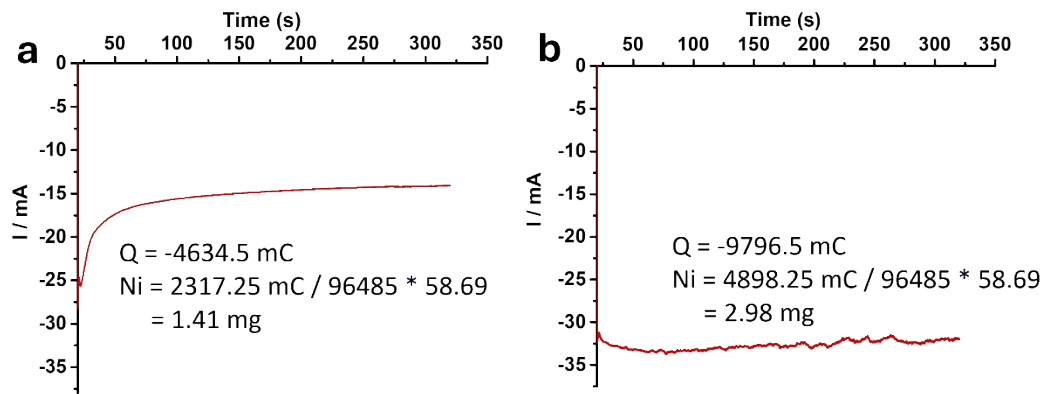


Figure S8. $I-t$ curve of electrodeposition process for (a) Ni/CP-TEA and (b) Ni/CP.

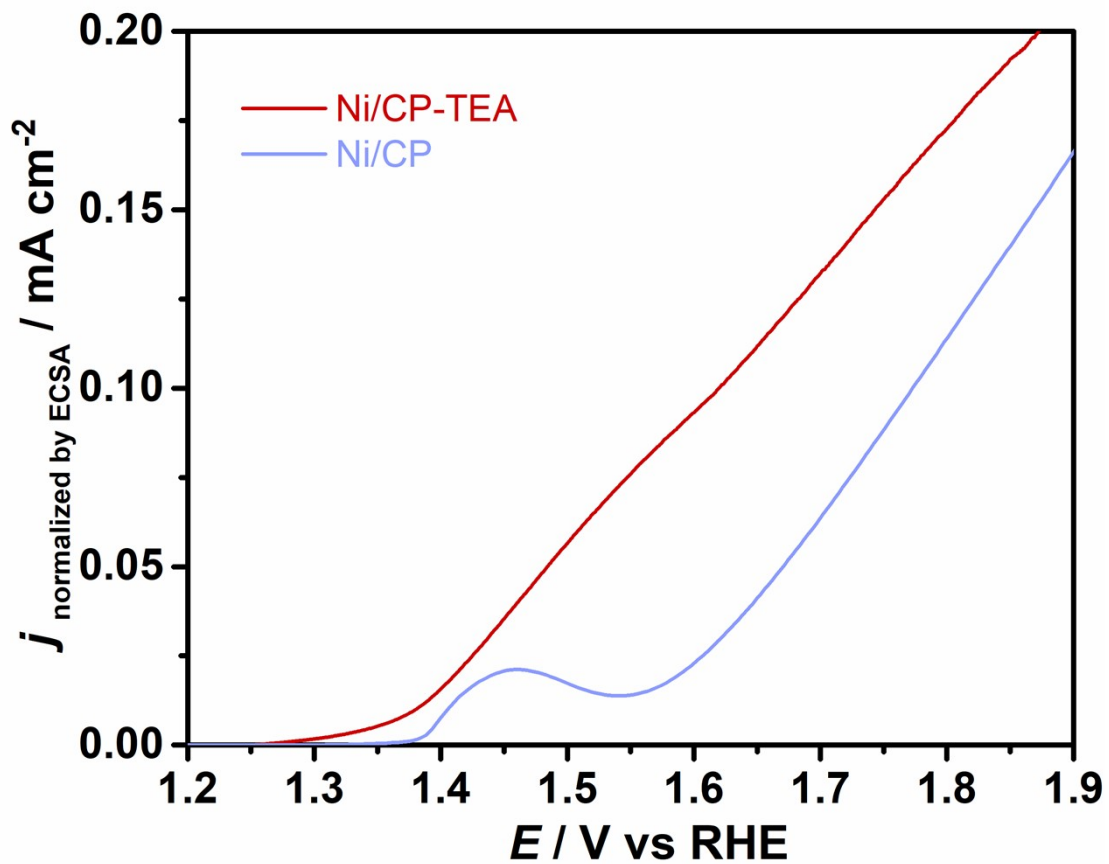


Figure S9. LSV curves normalized by ECSA of Ni/CP-TEA and Ni/CP.

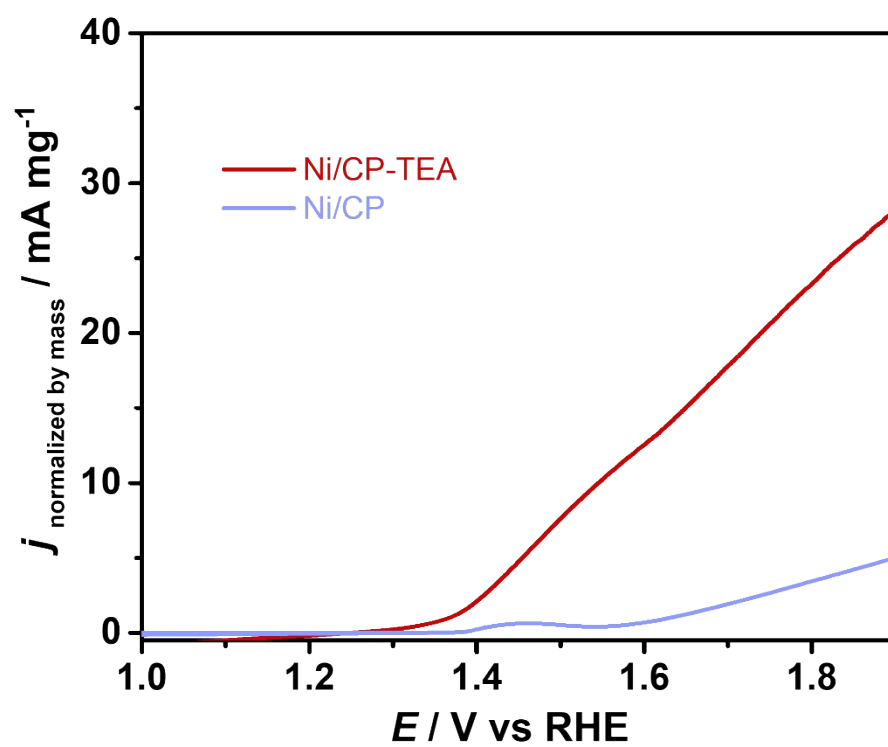


Figure S10. LSV curves normalized by catalyst mass of Ni/CP-TEA and Ni/CP.

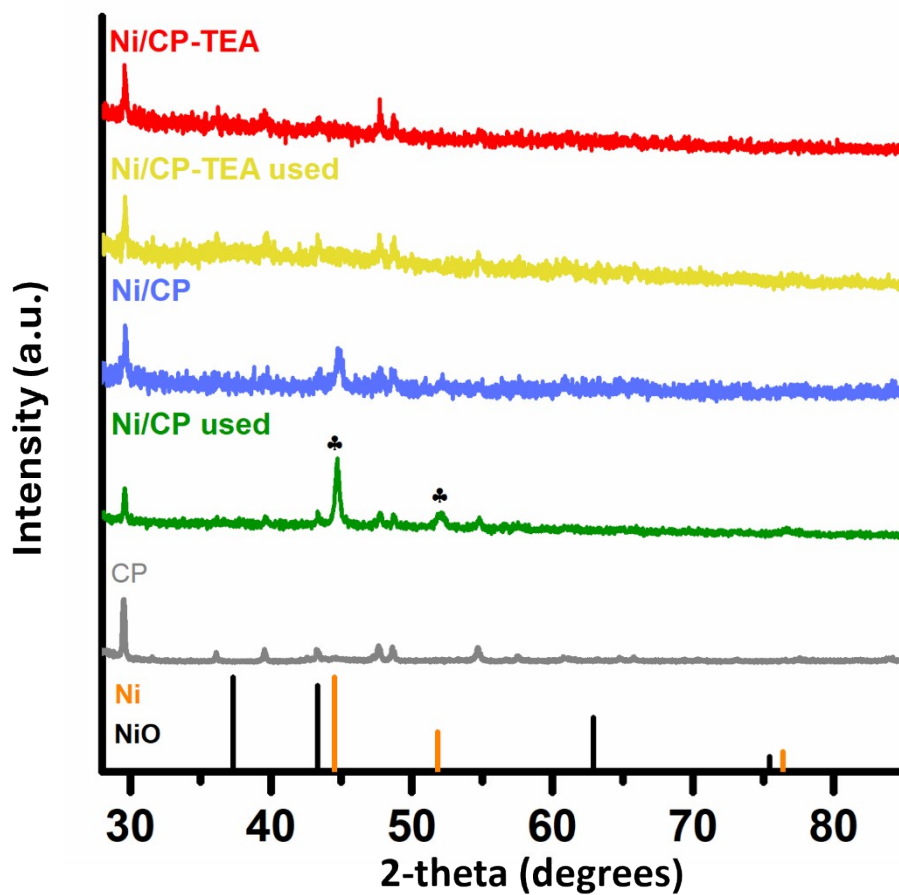


Figure S11. XRD pattern of CP, used Ni/CP-TEA and used Ni/CP. NiO: PDF# 00-004-0835; Ni: PDF# 01-071-4655.

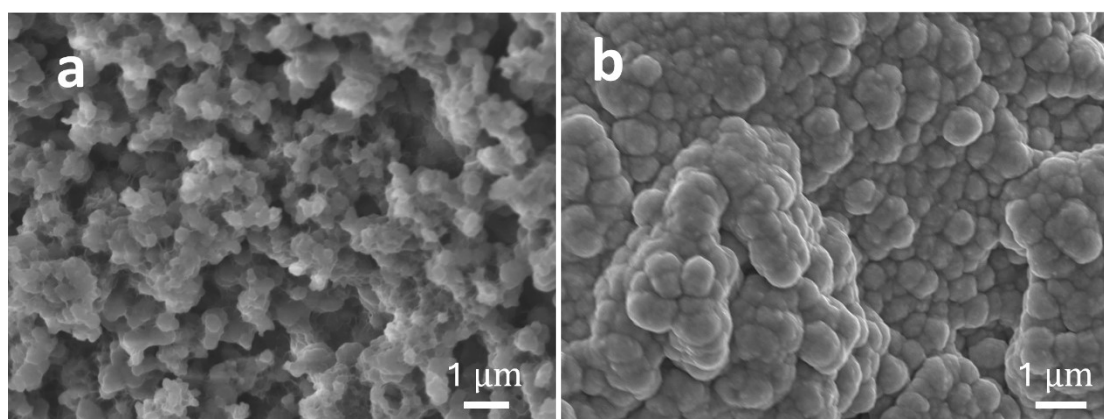


Figure S12. FESEM images of (a) used Ni/CP-TEA and (b) used Ni/CP

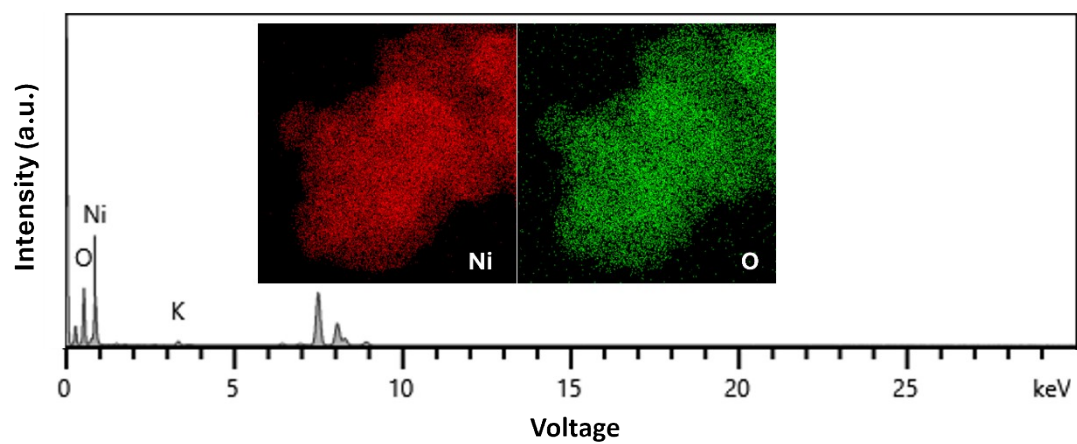


Figure S13. EDX spectrum of used Ni/CP-TEA and insert is related EDX elemental mapping.

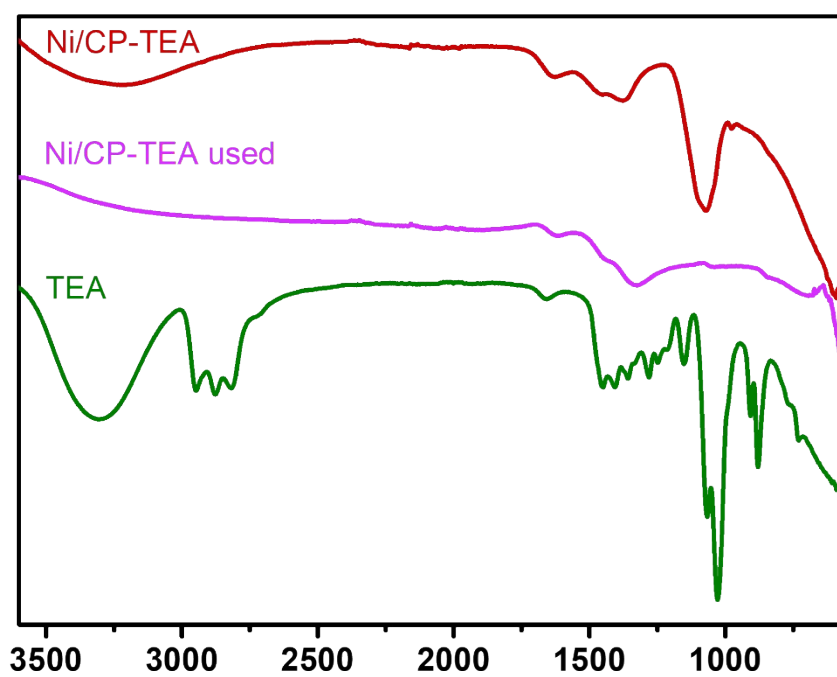


Figure S14. FTIR spectra of fresh Ni/CP-TEA, used Ni/CP-TEA and TEA.

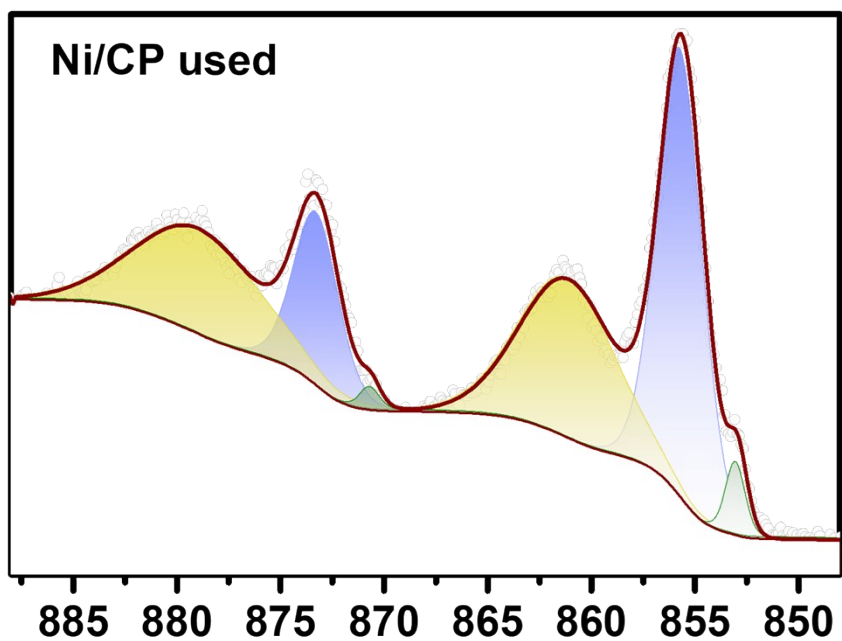


Figure S15. XPS spectra of Ni 2*p* region of used Ni/CP.

Table S1. Surface atomic concentration (at%) of the Ni/CP-TEA determined by XPS survey spectra with different etching times.

Etching time (s)	Ni Atomic (at%)	N Atomic (at%)
0	11.6	2.0
20	18.9	0.7
40	20.3	0.5
60	23.0	0.1
100	24.1	0.1

Table S2. Comparison of OER performance of Ni/CP-TEA with different Ni-based OER electrocatalysts.

	Electrolyte (KOH)	j (mA·cm ⁻²)	Overpotential (mV vs RHE)	Stability	Tafel slope (mV/Dec)	Ref
Ni/CP-TEA	0.1	10	320	20 h	-	This work
Ni-NiO/N-rGO	0.1	10	240	11 h	43	2
Ni-N ₄ /GHSs/Fe-N ₄	0.1	10	390	600 cycles (CV)	81	3
Zn _x Ni _{1-x} Co ₂ O ₄ /NCNTs	0.1	10	410	100 cycles (CV)	118.3±3	4
Ni-doped ALOOH NFs	0.1	10	320	7000 S	-	5
MIL-88A/Ni(OH) ₂ -CC	0.1	10	352	40 h	46.1	6
La(Co _{0.71} Ni _{0.25}) _{0.96} O _{3-δ}	0.1	10	324	10 h	71	7
RuO ₂	0.1	10	366	2000 cycles	69	8
NG-CoSe ₂	0.1	10	360	2000 cycles	40	8
RGO-Ni-Fe LDH	0.1	10	250	4000 s	33	9
NiO _x	1	10	430	2 h	-	10
NiO _x /Ni	1	10	390	20000 s	-	11
Ni ₃ N-NiMoN	1	10	277	20 h	118	12
Ni/N-CNT	1	10	590	-	138	13
N-NiMoO ₄ /NiS ₂	1	10	283	20 h	44.3	14
HCM@Ni-N	1	10	304	12 h	76	15
N-CoFe-OxHy	1	10	253	24 h	41	16
hNi ₃ N	1	10	325	30 h	50	17
FeOOH/Ni ₃ N	1	10	244	50 h	65	18
Ni SAs@S/N-CMF	1	10	285	60 h	50.8	19
Co-Ni (trace)/NCNTs	1	10	337	20000 s	94	20
Ni-Co _x B@BNC	1	10	274	24 h	80	21
Ni-P	1	10	300	10 h	64	22
Ni-MOF@Fe-MOF	1	10	265	1000 cycles (CV)	82	23
Ir-NiO	1	10	215	10 h	38	24
S-NiFe ₂ O ₄ /NF	1	10	267	24 h	36.7	25
Ni/Ni-N _{0.28} /NF	1	20	320	50 h	85	26
Ni ₃ N	1	52.3	350	18 h	45	27

References

1. L. Trotochaud, S. L. Young, J. K. Ranney and S. W. Boettcher, *J Am Chem Soc*, 2014, 136, 6744-6753.
2. X. Liu, W. Liu, M. Ko, M. Park, M. G. Kim, P. Oh, S. Chae, S. Park, A. Casimir, G. Wu and J. Cho, *Advanced Functional Materials*, 2015, 25, 5799-5808.
3. J. Chen, H. Li, C. Fan, Q. Meng, Y. Tang, X. Qiu, G. Fu and T. Ma, *Adv Mater*, 2020, 32, e2003134.
4. X. T. Wang, T. Ouyang, L. Wang, J. H. Zhong and Z. Q. Liu, *Angew Chem Int Ed Engl*, 2020, 59, 6554–6561.
5. Y. Zhou and H. C. Zeng, *ACS Sustainable Chemistry & Engineering*, 2019, 7, 5953-5962.
6. Z. Qian, K. Wang, K. Shi, Z. Fu, Z. Mai, X. Wang, Z. Tang and Y. Tian, *Journal of Materials Chemistry A*, 2020, 8, 3311-3321.
7. A. Vignesh, M. Prabu and S. Shanmugam, *ACS Appl Mater Interfaces*, 2016, 8, 6019-6031.
8. X. C. Min-Rui Gao, Qiang Gao, Yun-Fei Xu, Ya-Rong Zheng, Jun Jiang, and Shu-Hong Yu, *ACS Nano*, 2014, 8, 3970–3978.
9. D.-c. Xia, L. Zhou, S. Qiao, Y. Zhang, D. Tang, J. Liu, H. Huang, Y. Liu and Z. Kang, *Materials Research Bulletin*, 2016, 74, 441-446.
10. C. C. McCrory, S. Jung, J. C. Peters and T. F. Jaramillo, *J Am Chem Soc*, 2013, 135, 16977-16987.
11. Y.-R. L. Guan-Qun Han, Wen-Hui Hu, Bin Dong,*, Xiao Li, Xiao Shang, Yong-Ming Chai, Yun-Qi Liu, Chen-Guang Liu, *Applied Surface Science*, 2015, DOI: 10.1016/j.apsusc.2015.10.097, 172–176.
12. A. Wu, Y. Xie, H. Ma, C. Tian, Y. Gu, H. Yan, X. Zhang, G. Yang and H. Fu, *Nano Energy*, 2018, 44, 353-363.
13. Y. Liu, H. Jiang, Y. Zhu, X. Yang and C. Li, *Journal of Materials Chemistry A*, 2016, 4, 1694-1701.
14. L. An, J. Feng, Y. Zhang, R. Wang, H. Liu, G.-C. Wang, F. Cheng and P. Xi, *Advanced Functional Materials*, 2019, 29, 1805298.
15. H. Zhang, Y. Liu, T. Chen, J. Zhang, J. Zhang and X. W. D. Lou, *Adv Mater*, 2019, 31, e1904548.
16. X. Chen, Z. Qiu, H. Xing, S. Fei and L. Ma, *ACS Applied Energy Materials*, 2021, 4, 8866-8874.
17. B. Ouyang, Y. Zhang, Z. Zhang, H. J. Fan and R. S. Rawat, *Small*, 2017, 13, 1604265.
18. J. Guan, C. Li, J. Zhao, Y. Yang, W. Zhou, Y. Wang and G.-R. Li, *Applied Catalysis B: Environmental*, 2020, 269, 118600.
19. Y. Zhao, Y. Guo, X. F. Lu, D. Luan, X. Gu and X. W. D. Lou, *Adv Mater*, 2022, 34, e2203442.
20. Y. Shi, J. Cai, X. Zhang, Z. Li and S. Lin, *International Journal of Hydrogen Energy*, 2022, 47, 7761-7769.
21. J. Ding, X. Zhu, H. Pei, S. He, R. Yang, N. Liu, R. Guo and Z. Mo, *International Journal of Hydrogen Energy*, 2023, 48, 17468-17477.
22. X.-Y. Yu, Y. Feng, B. Guan, X. W. Lou and U. Paik, *Energy & Environmental Science*, 2016, 9, 1246-1250.
23. K. Rui, G. Zhao, Y. Chen, Y. Lin, Q. Zhou, J. Chen, J. Zhu, W. Sun, W. Huang and S. X. Dou, *Advanced Functional Materials*, 2018, 28, 1801554
24. Q. Wang, X. Huang, Z. L. Zhao, M. Wang, B. Xiang, J. Li, Z. Feng, H. Xu and M. Gu, *J Am Chem Soc*, 2020, 142, 7425-7433.
25. J. Liu, D. Zhu, T. Ling, A. Vasileff and S.-Z. Qiao, *Nano Energy*, 2017, 40, 264-273.
26. J. Shen, X. Zheng, L. Peng, G. I. N. Waterhouse, L. Tan, J. Yang, L. Li and Z. Wei, *ACS Applied Nano Materials*, 2020, 3, 11298-11306.
27. K. Xu, P. Chen, X. Li, Y. Tong, H. Ding, X. Wu, W. Chu, Z. Peng, C. Wu and Y. Xie, *J Am Chem Soc*, 2015, 137, 4119-4125.